Mechanism and Kinetics of the Water-Assisted Formic Acid + OH Reaction under Tropospheric Conditions

ARTICLE *in* THE JOURNAL OF PHYSICAL CHEMISTRY A · MAY 2011

Impact Factor: 2.69 · DOI: 10.1021/jp201517p · Source: PubMed

3 AUTHORS, INCLUDING:

Cristina Iuga
Metropolitan Autonomous University
43 PUBLICATIONS **342** CITATIONS

SEE PROFILE

Juan Raul Alvarez-Idaboy
Universidad Nacional Autónoma de México
121 PUBLICATIONS **2,177** CITATIONS

SEE PROFILE

THE JOURNAL OF PHYSICAL CHEMISTRY A

ARTICLE

pubs.acs.org/JPCA

Mechanism and Kinetics of the Water-Assisted Formic Acid + OH Reaction under Tropospheric Conditions

Cristina Iuga,[*,†,‡] J. Raul Alvarez-Idaboy,[*,†,§] and Annik Vivier-Bunge[§]

[†]Facultad de Química, Departamento de Física y Química Teórica, Universidad Nacional Autónoma de México, 04510 México D.F., Mexico

[‡]Departamento de Ciencias Básicas, Universidad Autónoma Metropolitana—Azcapotzalco, 02200 México D.F., Mexico

[§]Departamento de Química, Universidad Autónoma Metropolitana—Iztapalapa, 09340 México D.F., Mexico

ABSTRACT: In this work, we have revisited the mechanism of the formic acid + OH radical reaction assisted by a single water molecule. Density functional methods are employed in conjunction with large basis sets to explore the potential energy surface of this radical—molecule reaction. Computational kinetics calculations in a pseudo-second-order mechanism have been performed, taking into account average atmospheric water concentrations and temperatures. We have used this method recently to study the single water molecule assisted H-abstraction by OH radicals (Iuga, C.; Alvarez-Idaboy, J. R.; Reyes, L.; Vivier-Bunge, A. *J. Phys. Chem. Lett.* **2010**, *1*, 3112; Iuga, C.; Alvarez-Idaboy, J. R.; Vivier-Bunge, A. *Chem. Phys. Lett.* **2010**, *501*, 11; Iuga, C.; Alvarez-Idaboy, J. R.; Vivier-Bunge, A. *Theor. Chem. Acc.* **2011**, *129*, 209), and we showed that the initial water complexation step is essential in the rate constant calculation. In the formic acid reaction with OH radicals, we find that the water—acid complex concentration is small but relevant under atmospheric conditions, and it could in principle be large enough to produce a measurable increase in the overall rate constant. However, the water-assisted process occurs according to a formyl hydrogen abstraction, rather than abstraction of carboxylic hydrogen as in the water-free case. As a result, the overall reaction rate constant is considerably smaller. Products are different in the water-free and water-assisted processes.

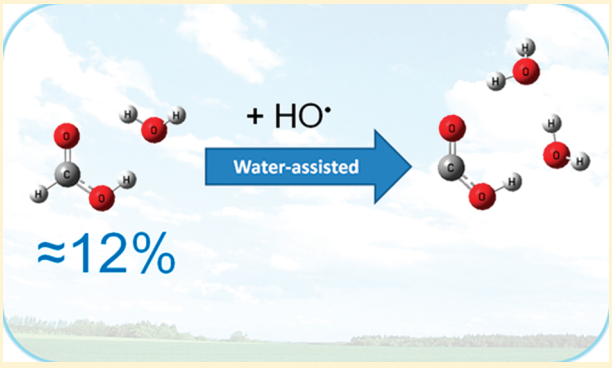

INTRODUCTION

There has been considerable speculation about the role of water complexes and hydrogen-bonded molecular complexes in the kinetics and dynamics of gas-phase free radical reactions. Indeed, in the troposphere, the water molecule could assist the chemical process by forming new intermolecular complexes and transition states. At relatively high temperatures such as those of the lower troposphere, weakly bonded complexes are not very stable[2] and their experimental characterization becomes particularly difficult. Under these conditions, theoretical studies can be very useful. One important property for which experimental information is scarce is the water complex concentration at room temperature. This information is needed because the extent to which molecular complexes affect the thermal balance and chemical balance of the atmosphere is ultimately determined by their atmospheric abundance.[2] The equilibrium between the free organic molecule and its water complex is strongly temperature dependent, with complex formation being favored at low temperatures. Thus, these species lifetimes are longer at cold temperatures. The result is that the associated species may act as reservoirs for the reactants that form them. At cold temperatures, these reservoirs can be transported to warmer remote regions of the atmosphere where they can thermally decompose back into their parent reactants, thus leading to observed concentrations that are much larger than expected.

It has been reported that formic acid (HCOOH) is the most abundant carboxylic acid in the troposphere.[3−8] Polluted atmospheric concentrations of formic acid of 10 ppb have been measured.[9] (typical concentrations in the parts per billion by volume (ppbv) range). Removal of formic acid from the atmosphere occurs mainly via rain out or reaction with the hydroxyl radical. Interestingly, formic acid has been found to account for a larger fraction of the acidity in remote areas than in urban areas, where sulfuric and nitric acids account for most of the acidity.[10] Moreover, researchers have found that water forms relatively strong complexes with both formic and acetic acids. Wine et al.[11] have suggested that, in the atmosphere, formation of this acid—water complex could affect the overall reactivity of OH with HCOOH. The reaction of formic acid with OH• radicals has been studied both experimentally[11−15] and theoretically,[16−18] and the reported reaction rate coefficients at 298 K are fairly consistent, ranging from 4.0×10^{-13} to 4.9×10^{-13} cm^3 molecule^{-1} s^{-1}. The rate coefficient was reported to be relatively temperature independent between 298 and 400 K.[11,14] Within experimental uncertainty, the temperature dependence of the rate coefficient is nearly zero.

Received: February 15, 2011
Revised: April 19, 2011
Published: April 29, 2011

The reaction can proceed via either an acid or a formyl H-abstraction channel. Because the radical intermediate formed decomposes rapidly to CO_2 and $H^{\bullet}$, it is difficult to determine the relative rates of the individual channels experimentally:

$$HCOOH + HO^{\bullet} \rightarrow HCOO^{\bullet} + H_2O \quad (I)$$

$$HCOOH + HO^{\bullet} \rightarrow {}^{\bullet}COOH + H_2O \quad (II)$$

In HCOOH the strength of the C−H bond is smaller than that of the O−H bond (the experimental bond dissociation energies (BDEs) are 96.2 ± 0.7 and 112.2 ± 3.1 kcal/mol, respectively).[19] Yet, kinetic studies performed by Wine et al.,[11] Jolly et al.,[13] and Singleton et al.[14] indicate that, at room temperature, the reaction pathway involving abstraction of the carboxylic hydrogen (I) dominates over the formyl hydrogen abstraction (II). Indeed, isotopic studies by Singleton et al.[14] showed that substitution of the carboxylic H by D has a very dramatic effect on the reactivity, whereas a similar substitution at the formyl group does not influence the reaction rate. These results suggest that reaction between the OH radical and the carboxylic hydrogen is considerably faster than the one between OH and the formyl hydrogen. However, the latter makes a small but significant contribution to the overall rate constant and it should be taken into account.

In addition, the reactivity of OH with the formic acid dimer is lower than that of the monomer, supporting the conclusion that the hydroxyl radical abstracts predominantly the carboxylic hydrogen.

It has been demonstrated that prereactive intermediates formed between OH and volatile organic compounds play an important role in atmospheric bimolecular reactions, and that they may have a key influence on the rate constant and on its dependence on temperature and pressure.[20−22] Galano et al.[16] reported a theoretical study of the OH + HCOOH reaction mechanism, pointing out the important influence, on the rate constant, of the reactant complex formation and of the quantum mechanical tunneling effect. More recently, three different theoretical publications by Anglada et al. focused on several prereactive complexes formed between formic acid and hydroxyl radicals[23] and on the reaction mechanism of the carboxylic hydrogen abstraction by OH.[17,18] The latter bring light to an unexpected reaction mechanism based on a proton coupled electron-transfer process (PCET), which can compete with a conventional hydrogen radical abstraction.

It is also interesting to point out that experimental results indicate that the rate coefficient of the formic acid + OH reaction is approximately 10 times smaller than the one for the HCHO + OH reaction.[24,25] Since the measured activation energy (E_a) of formaldehyde + OH is about 0, one would expect a larger and positive E_a value for formic acid + OH, in disagreement with experimental values.[11,14]

In recent work we have shown[26] that, in the case of bimolecular processes that yield a single product (A + B → C), it is not always possible to extrapolate results obtained in chamber experiments to processes at atmospheric concentrations. Under these pseudo-first-order conditions, the relative equilibrium concentrations depend strongly on the concentration of the excess reactant.

Previous studies[27−29] have examined complexes of water and formic acid using both theoretical and experimental methods. Theoretical work has also been performed on the formic acid + OH reaction in the presence of a single water molecule,[30] to investigate a possible catalytic effect. However, in recent work on the acetaldehyde + OH and glyoxal + OH reactions,[1] we have shown that, although in the water-assisted model the transition state barrier is considerably lowered by hydrogen bonds involving the water molecule, the amount of water complex formed is so small (≈0.02%) that there is no detectable rate constant increase. Indeed, it is not correct to calculate the effective rate constant as a bimolecular rate: it should be calculated in a pseudo-second-order mechanism, taking into account average atmospheric water concentrations and temperatures. Other authors have recently used our methodology to study the water-assisted glyoxal + HOO reaction.[31]

Unlike glyoxal and acetaldehyde, the amount of formic acid−water complex in equilibrium with free formic acid at room temperature is not negligible (about 12%), and formic acid could thus be a candidate for one-water-molecule catalysis. In this work, we report accurate computational kinetics calculations on the gas-phase water-free and water-assisted formic acid + OH reactions under tropospheric conditions, aiming to clarify whether the presence of one water molecule modifies the reaction rate constant. Energy profiles are calculated for paths corresponding to reactions I and II. Arrhenius parameters, tunneling corrections, and rate constants are obtained and compared with the available experimental data.

METHODOLOGY

Electronic structure calculations have been performed with the Gaussian 03 program using the M05-2X[32] method, in conjunction with the 6-311++G(d,p) basis set. Frequency calculations were performed for all stationary points at the same level of theory as the geometry optimization, and local minima were identified. The M05-2X functional has been recommended for kinetics calculations by their developers,[33] and it has been also successfully used to that purpose by independent authors.[34−41] In the particular cases of refs 34 and 36 the correspondence between M05-2X and experimental results is better than the one obtained using highly correlated wave function methods.

In this work, relative energies are calculated with respect to the sum of the separated reactants. We have reported both ΔE and ΔG energetic profiles for the water-free and water-assisted reactions. Unrestricted calculations are used for open shell systems. Zero-point energies (ZPEs) and thermal corrections to the energy (TCE) are included in the determination of energy barriers. Since the rate coefficient analysis includes the influence of entropic factors on the reactivity, we consider that ΔG profiles provide a more complete approach to chemical reactions than mere energetic considerations. The entropy changes, as well as the tunneling effect, could lead to a site reactivity different from the one expected by taking into account only ZPE corrected energy barriers.

Rate constants have been computed using conventional transition state theory (TST)[42−44] as implemented in TheRate program[45] at the Computational Science and Engineering Online Web site (www.cseo.net).[46] The equilibrium constants were also obtained using the same program. The energy values, partition functions, and thermodynamic data were taken from the quantum mechanical calculations. Tunneling effects are accounted for using the zero curvature tunneling (ZCT) method.[47]

In the water-assisted reactions, we have used 100% humidity water concentration at each temperature. This methodology has

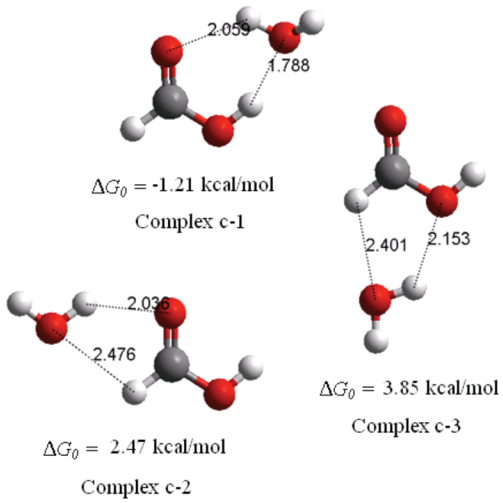

Figure 1. Water−formic acid complexes. Free energy values are given at 298 K.

been successfully used previously in theoretical work on water−molecule complexes.[1,48]

Counterpoise corrections (CP) to the basis set superposition error (BSSE) have not been included, since it has been recently demonstrated that, for a large variety of systems including •OH hydrogen abstraction from formaldehyde, CP corrected energies systematically differ more from the complete basis set extrapolated values than the uncorrected ones.[49,50] Moreover, it has been shown that counterpoise corrections tend to overestimate the BSSE.[51]

RESULTS AND DISCUSSION

Electronic molecular calculations of the potential energy surfaces in the water-free and water-assisted formic acid + OH reactions along the different channels were performed. First, water complexes involving water and formic acid have been studied. In a second step, energy profiles for both water-free and water-assisted reactions have been calculated. Finally, the rate constants for the elementary reactions have been computed using classical transition state theory in a pseudo-second-order methodology.

Water Complexes. The potential energy surface for the formation of formic acid−water complexes was carefully searched, and all stationary structures were identified. Water can attach to formic acid in three positions, forming cyclic radical−molecule complexes that are held together by hydrogen bonding (Figure 1).

The most stable intermolecular complex (c-1) adopts a six-member-ring-like configuration, while c-2 and c-3 structures are five-membered. In the c-1 complex, both water and formic acid act as hydrogen donor and acceptor, resulting in two relatively strong hydrogen bonds (the water oxygen atom binds to the carboxylic H atom, while one of the water hydrogens binds to the carbonyl oxygen). In the c-2 conformation, the water acts as hydrogen donor to the carbonyl oxygen of the formic acid. In this structure, the water is situated on the opposite side of the carbonyl group relative to the O−H group. In a third conformation (c-3), the water molecule acts as a hydrogen donor again, only this time to the oxygen bound to the carboxylic formic acid hydrogen. The latter is the most weakly bound of the three

Table 1. Calculated Equilibrium Constant K_0, in cm^3 molecule^{-1}, of Water Complexes between 250 and 330 K (Formic Acid Concentration = 1 × 10^{12} molecules cm^{-3})

T (K)	complex c-1	complex c-2	complex c-3
250	3.84×10^{-18}	1.33×10^{-21}	7.69×10^{-23}
260	1.79×10^{-18}	9.40×10^{-22}	6.13×10^{-23}
270	8.79×10^{-19}	6.83×10^{-22}	4.98×10^{-23}
280	4.57×10^{-19}	5.09×10^{-22}	4.13×10^{-23}
290	2.49×10^{-19}	3.88×10^{-22}	3.47×10^{-23}
300	1.41×10^{-19}	3.02×10^{-22}	2.96×10^{-23}
310	8.33×10^{-20}	2.40×10^{-22}	2.56×10^{-23}
320	5.09×10^{-20}	1.93×10^{-22}	2.24×10^{-23}
330	3.21×10^{-20}	1.58×10^{-22}	1.98×10^{-23}

conformations. Complex c-1 is the only formic acid−water complex that has been observed experimentally.[29,52]

The complexation energy (ΔE_0) and the Gibbs free energy (ΔG_0) are calculated as

$$\Delta E_0 = E_{\text{complex}} - (E_{\text{HCOOH}} + E_{\text{water}}) + \Delta(\text{ZPE})$$

$$\Delta G_0 = G_{\text{complex}} - (G_{\text{HCOOH}} + G_{\text{water}})$$

The calculated optimized geometries of the formic acid complexes with one water molecule are in good agreement with previously reported calculations. As expected, the hydrogen bonds in which the formic acid acts as a hydrogen donor to the water are shorter than the hydrogen bonds where the water donates a hydrogen atom to the carbonyl oxygen atom, explaining why c-1 is the most stable complex.[48]

No experimental data are available for the amount of acid−water complex formed under tropospheric conditions, but it can be estimated theoretically using the following expression:

$$[\text{complex}] = K_0[\text{acid}][\text{water}] \quad (1)$$

where K_0 is calculated from quantum chemistry results. The water concentration in the gas phase is strongly dependent on the temperature of the atmosphere. The amount of water vapor also generally decreases with increasing altitude. Thus, different possible atmospheric water concentrations were used depending on temperature, in order to estimate the effect of the relative air humidity on the acid−water complex concentration. The acid concentration was taken to be 1 × 10^{12} molecules cm^{-3}, which is reasonable in a polluted environment.[3−8]

Equilibrium constants K_0 for the formation of the three identified formic acid−water complexes, in the 250−330 K range and at 100% humidity, are reported in Table 1.

Corresponding estimated concentrations of the c-1 complex between 250 and 330 K are reported in Table 2. These concentrations represent the upper limit for the complex at each temperature.

The proportion in which the formic acid is expected to be complexed with a water molecule was estimated in percentage according to the following:

$$\% \text{ complex} = \frac{[\text{complex}]}{[\text{HCOOH}]} \times 100$$

and it is also given in Table 2.

From the data in Table 2 it can be seen that, at 298 K, a fraction of approximately 12% of the initial amount of formic acid is complexed with water to form the c-1 complex. Only 0.02 and

dx.doi.org/10.1021/jp201517p |J. Phys. Chem. A 2011, 115, 5138–5146

Table 2. Calculated Concentrations of the c-1 Complex between 250 and 330 K, and Complex Percent for c-1

T (K)	c-1 concentration	c-1 (%)
250	8.46×10^{10}	8.46
260	9.73×10^{10}	9.73
270	1.11×10^{11}	11.1
280	1.17×10^{11}	11.7
290	1.19×10^{11}	11.9
300	1.20×10^{11}	12.0
310	1.21×10^{11}	12.1
320	1.21×10^{11}	12.1
330	1.21×10^{11}	12.1

0.002% form c-2 and c3, respectively. As discussed in ref 1, the methodology used in our work yields a calculated percent for water dimer formation of 0.7%, in very good agreement with experimental findings.[53] Thus, the c-1 formic acid−water complex is predicted to be considerably more strongly complexed than the water dimer. Of course, the overall water dimer concentration will still, in general, be much larger than the formic acid−water complex concentration, since the amount of water is orders of magnitude larger than that of formic acid.

Water-Free Reaction Geometries and Energies. We use here the term "water-free reaction" to express the reaction between formic acid and an OH radical in a dry atmosphere; i.e., no water molecule is involved.

In the water-free reaction, two different channels are possible, corresponding to abstraction of either the carboxylic or the formyl hydrogen atom. Reaction I produces water and a formyloxyl radical (HCOO), while reaction II leads to the formation of water plus hydroxyformyl radical (HOCO).

In both cases, the reaction path takes place in two steps, with the first one leading to the formation of the prereactive complex (or reactant complex, RC) and the second one yielding the corresponding radical and water. For the carboxylic hydrogen abstraction, the equations representing these steps are

Step 1:

$$\mathrm{HCOOH} + \mathrm{OH}^{\bullet} \underset{k_{-1}}{\overset{k_1}{\rightleftharpoons}} [\mathrm{HCOOH}\cdots\mathrm{HO}]^{\bullet}$$

Step 2:

$$[\mathrm{HCOOH}\cdots\mathrm{HO}]^{\bullet} \xrightarrow{k_2} \mathrm{HCOO}^{\bullet} + \mathrm{H_2O}$$

while for the formyl hydrogen abstraction, they are

Step 1:

$$\mathrm{HCOOH} + \mathrm{OH}^{\bullet} \underset{k_{-1}}{\overset{k_1}{\rightleftharpoons}} [\mathrm{HCOOH}\cdots\mathrm{HO}]^{\bullet}$$

Step 2:

$$[\mathrm{HCOOH}\cdots\mathrm{HO}]^{\bullet} \xrightarrow{k_2} {}^{\bullet}\mathrm{COOH} + \mathrm{H_2O}$$

In addition, two reaction paths are possible for each type of abstraction. The fully optimized structures of the stationary points involved in the water-free carboxylic H-abstraction (Ia and Ib) and formyl H-abstraction (IIa and IIb) pathways are presented in Figures 2 and 3 (R = reactants, RC = prereactive complex, TS = transition state, PC = product complex, P = products). Relative energies are calculated with respect to the sum of the separated reactants at 0 K, and free energies are given in Figures 2 and 3 under each structure. Energies and free energies are reported in Table 3: ΔE_1 ($\Delta E_1 = E^{\mathrm{RC}} - E^{\mathrm{R}}$) is the prereactive complex stabilization energy, which also represents the barrier height for the unimolecular elementary reaction in the first step of the complex mechanism; $\Delta E_{\mathrm{eff}}^{\ddagger}$ is the effective activation energy ($\Delta E_{\mathrm{eff}}^{\ddagger} = E^{\mathrm{TS}} - E^{\mathrm{R}}$); ΔE is the reaction energy ($\Delta E = E^{\mathrm{P}} - E^{\mathrm{R}}$).

Both carboxylic H-abstraction paths (Figure 2) initiate at the same prereactive complex. They may occur either by a direct proton transfer from formic acid to the OH radical (HAT) or, as first discussed by Anglada et al.,[18] by a proton-coupled electron transfer (PCET). Geometries and free energies are quite different for these two paths, yet they both lead to the same final product complex. In the gas phase HCOOH + OH reaction, the PCET mechanism is energetically favored.

In the formyl H-abstraction (Figure 3), two different transition states are identified, depending on the OH approach. In path IIa, the OH hydrogen atom approaches the carbonyl oxygen, while in path IIb it approaches the carboxylic oxygen. Although distinctively different in geometry, both conformations have very similar free energies, and they lead to the same final product complex. As barriers are energetically close, one should see if they are separated from one another by either a high or a low barrier. In this particular case, TS-IIa and TS-IIb seem to be separated by a very small barrier due to almost free rotation around the O···H incipient bond (between the OH oxygen atom and the transferred H atom). The two transition states would then be coupled to an anharmonic transition state, and their rate constants should not be added. Hence, we choose the one with the largest rate constant. In the section Water-Free Reaction Kinetics we shall see that path IIa is actually slightly faster than IIb, due to a larger transmission coefficient. Thus, for the overall rate constant kinetics calculation, path IIa will be used.

Water-Free Reaction Kinetics. Rate constants for the water-free formic acid + OH reactions have been determined using transition state theory. Assuming that the prereactive concentration is stationary, the effective rate constant k^{eff} for each individual channel is calculated as[54]

$$k^{\mathrm{eff}} = \sigma K_1 \kappa k_2 \qquad (2)$$

where κ is the tunneling correction, σ is the reaction path degeneracy which, in this case, is equal to 1, K_1 is the equilibrium constant for step 1, and k_2 is the rate constant for step 2. See Table 4.

If all the reaction paths are taken into account (carboxylic H-abstraction + formyl H-abstraction), it is possible to write the overall rate constant, k^{overall}, as the sum of the fastest channel I and II individual rate constants. Thus, the overall rate constant (carboxylic H-abstraction + formyl H-abstraction) in the gas phase at 298 K is calculated to be the sum of the Ib and IIa effective rate constants: 4.49×10^{-13} cm^3 molecule^{-1} s^{-1}, in excellent agreement with reported experimental rate constants ($(3.2 \pm 1)-(4.9 \pm 1.2) \times 10^{-13}$ cm^3 molecule^{-1} s^{-1}). (See Table 5.) The carboxylic H-abstraction is clearly predominant, and formyl H-abstraction represents about 16.3%, in agreement

dx.doi.org/10.1021/jp201517p |J. Phys. Chem. A 2011, 115, 5138–5146

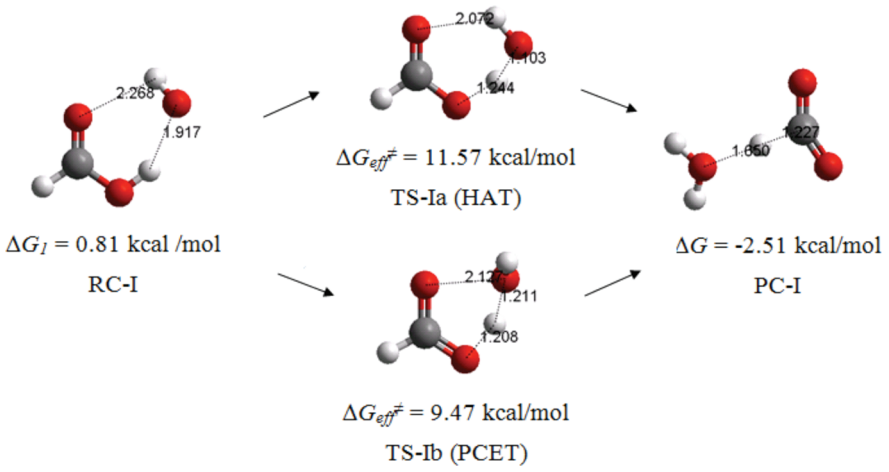

Figure 2. Water-free carboxylic H-abstraction pathways (Ia and Ib). Free energy values are given at 298 K.

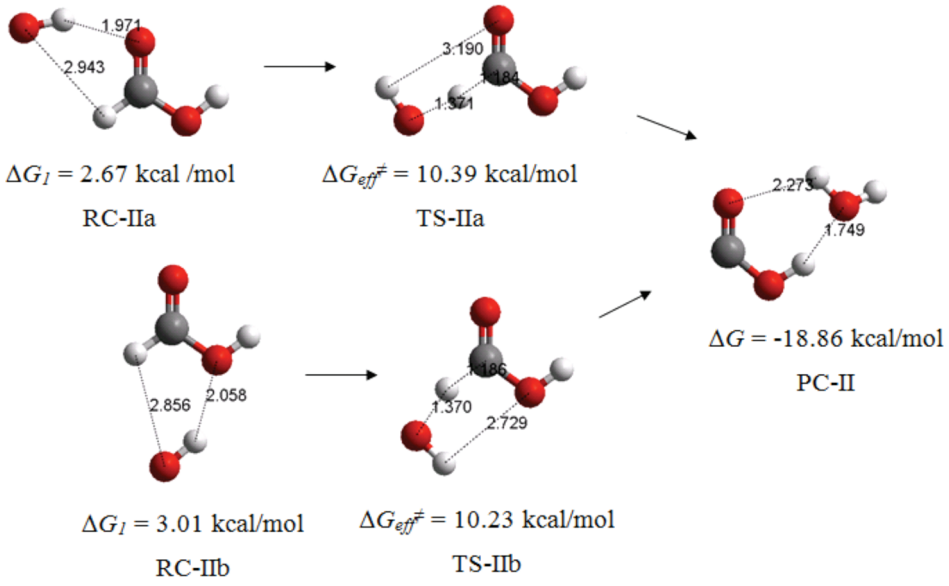

Figure 3. Water-free formyl H-abstraction II. Free energy values are given at 298 K.

Table 3. Relative Electronic Energies (Including Zero-Point Energies) and Gibbs Free Energies (Including Thermal Corrections), in kcal/mol, in the Water-Free Formic Acid + OH Reaction

path	ΔE_1	$\Delta E_{eff}^{\ddagger}$	ΔE	ΔG_1	$\Delta G_{eff}^{\ddagger}$	ΔG
Ia (HAT)	−6.78	3.20	−2.81	0.81	11.57	−3.58
Ib (PCET)	−6.78	0.76	−2.81	0.81	9.47	−3.58
IIa	−4.35	2.99	−16.57	2.67	10.39	−17.24
IIb	−2.90	2.60	−16.57	3.01	10.23	−17.24

Table 4. Calculated Equilibrium Constants (in cm^3 $molecule^{-1}$), Rate Constants k^{eff} (in cm^3 $molecule^{-1}$ s^{-1}), and Tunneling Corrections (κ) at 298 K, in the Water-Free Formic Acid + OH Reactions

path	K_1	κ	k_2	k^{eff}
Ia (HAT)	1.05×10^{-20}	22.8	7.96×10^{4}	1.90×10^{-14}
Ib (PCET)	1.05×10^{-20}	13.1	2.76×10^{6}	3.78×10^{-13}
IIa	4.51×10^{-22}	11.7	1.35×10^{7}	7.14×10^{-14}
IIb	2.53×10^{-22}	8.7	3.14×10^{7}	6.94×10^{-14}

with experimental data (8−15%). The choice of the M05-2X/6-311++G(d,p) method for the calculation was based on these results, as well as on our previous experience using this method.[34,36,37,40]

Water-Assisted Reaction Geometries and Energies. As we have pointed out in previous work,[1] water could act as an intramolecular third body to efficiently stabilize the OH···HCOOH complex, thus lowering the reaction barrier. However, this is not a sufficient condition to conclude that a single water molecule accelerates the reaction.

In order to examine the possible catalytic effect of water vapor on the formic acid + OH gas phase reaction, we have explored

dx.doi.org/10.1021/jp201517p |J. Phys. Chem. A 2011, 115, 5138–5146

the potential energy surface and the mechanisms involved in the addition of one H_2O molecule to the system. Since the simultaneous collision of three molecules is very improbable, in the water-assisted reaction the termolecular mechanism is ruled out. Hence, the most probable mechanism consists of two consecutive bimolecular elementary steps, possibly followed by unimolecular steps. In the water-assisted formic acid + OH reaction, the following three steps have been considered:

Step 0:

$$HCOOH + H_2O \underset{k_{-0}}{\overset{k_0}{\rightleftharpoons}} [HCOOH\cdots H_2O]$$

Step 1:

$$[HCOOH\cdots H_2O] + HO^\bullet \underset{k_{-1}}{\overset{k_1}{\rightleftharpoons}} [HCOOH\cdots H_2O\cdots HO]^\bullet$$

Step 2:

$$[HCOOH\cdots H_2O\cdots HO]^\bullet \xrightarrow{k_2} \text{products}$$

Table 5. Reaction Rate Constants, in cm^3 $molecule^{-1}$ s^{-1} as a Function of Temperature in a Water-Free Atmosphere

T (K)	k^{eff}(Ib (PCET))	k^{eff}(IIa)	$k^{overall}_{water\text{-}free}$
250	1.02×10^{-12}	7.79×10^{-14}	1.08×10^{-12}
260	7.86×10^{-13}	7.39×10^{-14}	8.60×10^{-13}
270	6.24×10^{-13}	7.15×10^{-14}	6.95×10^{-13}
280	5.12×10^{-13}	7.05×10^{-14}	5.82×10^{-13}
290	4.28×10^{-13}	7.06×10^{-14}	4.99×10^{-13}
300	3.67×10^{-13}	7.16×10^{-14}	4.39×10^{-13}
310	3.20×10^{-13}	7.38×10^{-14}	3.94×10^{-13}
320	2.84×10^{-13}	7.58×10^{-14}	3.60×10^{-13}
330	2.56×10^{-13}	7.89×10^{-14}	3.35×10^{-13}

Step 0 is the reversible formation of a complex between formic acid and a water molecule; in step 1, the termolecular water−acid−OH prereactive complex is formed reversibly; the last step is the irreversible formation of the products.

In this work, we have considered the H_2O-assisted reaction that starts by the formation of the most stable water−formic acid complex (c-1). Four prereactive complexes were then optimized: two for the carboxylic channel and two for the formyl channel.

The fully optimized structures of the stationary points involved in the water-assisted carboxylic H-abstraction (Ia and Ib) and formyl H-abstraction (IIa and IIb) pathways (prereactive complexes, transition states, and product complexes) are presented in Figures 4 and 5. Free energies, relative to reactants, are also indicated in the figures.

As in the water-free case, two possible mechanisms are possible for the carboxylic hydrogen abstraction: path Ia (HAT) and path Ib (PCET). Each of them initiates with a different prereactive complex, depending on whether the original water molecule in c-1 moves closer to the formyl oxygen or the carboxylic hydrogen of formic acid. Actually, the latter forms the most stable RC with the OH radical. The PCET transition state is more endergonic than the HAT transition state, and its effective barrier is then larger than that for the HAT path. Thus, in contrast to the water-free case, the PCET mechanism is not favored.

In the formyl H-abstraction (Figure 5), again two prereactive complexes are found. The c-1 complex is not modified as much as in paths Ia and Ib. Actually the water molecule stays approximately in the same position as in c-1, and the OH radical attacks from two different directions: in IIa, the OH hydrogen atom points toward the formic acid carbonyl O atom, while in IIb it points toward the hydroxyl oxygen. The former is favored. Transition states have similar energies, both are considerably smaller than in paths I, and the final product complex is very stable.

Relative energies are calculated with respect to the sum of the separated reactants at 0 K, and they are reported in Table 6.

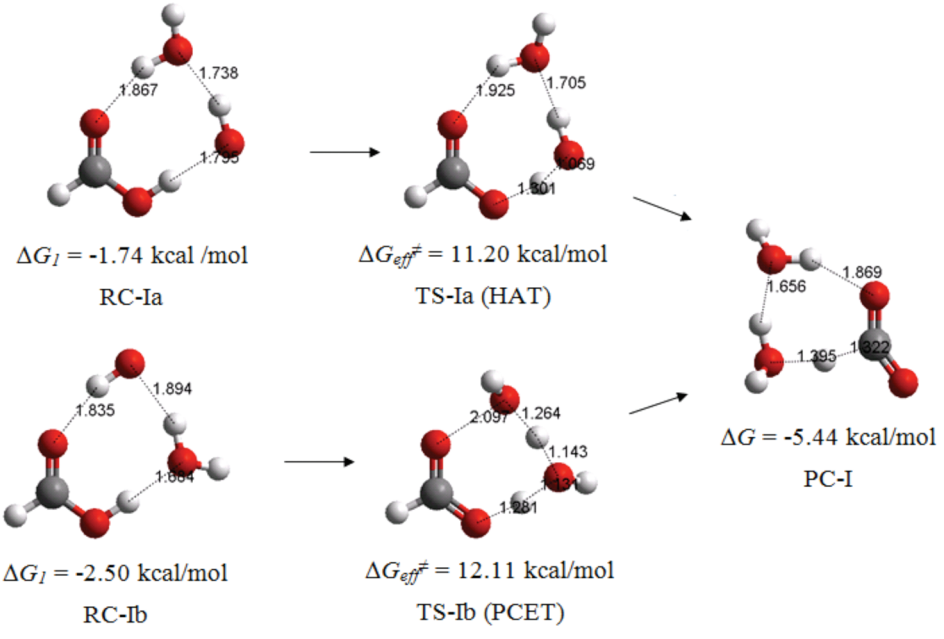

Figure 4. Water-assisted carboxylic H-abstraction paths (Ia and Ib). Free energy values are given at 298 K.

dx.doi.org/10.1021/jp201517p |J. Phys. Chem. A 2011, 115, 5138–5146

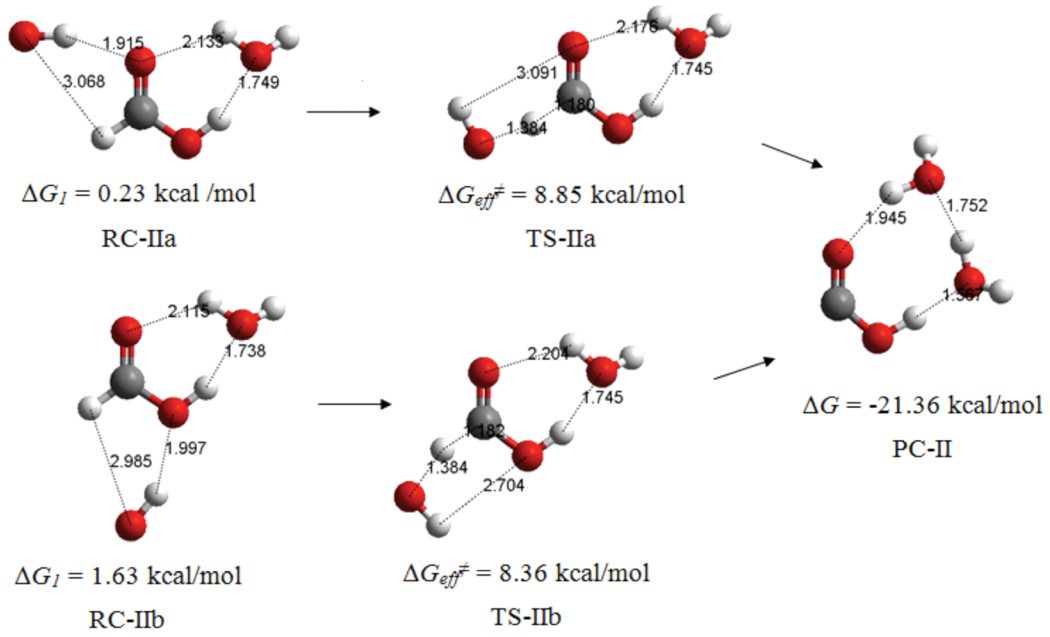

Figure 5. Water-assisted HCOOH + OH formyl H-abstraction (IIa and IIb). Free energy values are given at 298 K.

Table 6. Relative Electronic Energies (including ZPE) and Gibbs Free Energies (Including TCE), in kcal/mol, in the Water-Assisted Formic Acid + OH Reaction

path	ΔE_0	ΔE_1	$\Delta E_{eff}^{\ddagger}$	ΔE	ΔG_0	ΔG_1	$\Delta G_{eff}^{\ddagger}$	ΔG
Ia (HAT)	−9.62	−17.81	−5.28	−22.05	−1.21	−1.74	11.20	−5.44
Ib (PCET)	−9.62	−18.60	−5.50	−22.05	−1.21	−2.50	12.11	−5.44
IIa	−9.62	−14.71	−7.10	−37.42	−1.21	0.23	8.85	−21.36
IIb	−9.62	−13.23	−7.69	−37.42	−1.21	1.63	8.36	−21.36

ΔE_0 and ΔG_0 refer to the binding energy between formic acid and a water molecule. The other terms in Table 6 have already been defined above.

The essential point here is that, while in the water-free case the PCET carboxylic hydrogen abstraction path was the overall most favored reaction channel, in the water-assisted reaction the carboxylic hydrogen is strongly involved in the c-1 complex, and it is therefore less available for reaction with an OH radical. Thus, free energy values point to a preference for a formyl hydrogen abstraction channel.

We note that, in this study, the product potential energy surface was not explored systematically, since any bound species that includes HCOO/HOCO and two water molecules will finally decompose into dissociated species via energy dissipating processes of the present exothermic reactions.

Water-Assisted Reaction Kinetics. In the water-assisted reaction, an additional elementary step, step 0, has to be included, and the effective rate constant is

$$k^{\text{eff}} = \sigma\kappa K_0 K_1 k_2 [\text{water}] \qquad (3)$$

where K_0 is equal to the equilibrium constant for the formation of the formic acid−water complex.

Under pseudo-first-order conditions, the relative equilibrium concentrations depend strongly on the concentration of the excess reactant, i.e., water. As in our previous work on the water-assisted acetaldehyde + OH and glyoxal + OH reactions,[1] the pseudo-second-order rate constant is calculated using the maximum possible water concentration (i.e., 100% humidity) at each temperature. This methodology has been successfully used previously in theoretical work on complexes of volatile organic compounds with water.[1]

Table 7. Calculated Equilibrium Constants (in cm^3 $molecule^{-1}$), Rate Constants k^{eff} (in cm^3 $molecule^{-1}$ s^{-1}) and Tunneling Corrections (κ), in Water-Assisted Formic Acid + OH Reactions, Calculated at 298 K and 100% Relative Air Humidity

path	K_0	K_1	κ	k_2	k^{eff}
Ia (HAT)	1.57×10^{-19}	1.00×10^{-19}	22.0	2.00×10^{3}	5.35×10^{-16}
Ib (PCET)	1.57×10^{-19}	3.65×10^{-19}	5.93	1.19×10^{2}	3.13×10^{-17}
IIa	1.57×10^{-19}	3.60×10^{-21}	8.38	3.00×10^{6}	1.09×10^{-14}
IIb	1.57×10^{-19}	3.42×10^{-22}	6.02	7.17×10^{7}	1.79×10^{-14}

Results are presented in Table 7.

Partial rate constant values confirm that the PCET channel, which was the fastest in the water-free case, becomes more than an order of magnitude smaller in the presence of water. Channel Ia is also much slower than any of the formyl channels. For these, the rate constants also decrease with respect to their values in the water-free reaction. Overall, while the H−C abstraction rate constant decreases by a factor of 7, the H−O abstraction rate constant decreases by a factor of 10^4. Thus, the result of water complexation is to dramatically decrease the H−O abstraction while slightly increasing the H−C abstraction and, as a consequence, the fraction of formic acid that is complexed with water reacts almost exclusively by H−C abstraction.

To calculate the overall rate constant (carboxylic H-abstraction + formyl H-abstraction) for the water-assisted fraction of the formic acid reaction at 298 K, it is necessary to analyze carefully the different paths. In the case of paths Ia and IIb (Figure 4), these mechanisms are fundamentally different, and moreover, the calculated rate constants differ by more than an

dx.doi.org/10.1021/jp201517p |J. Phys. Chem. A 2011, 115, 5138–5146

Table 8. Water-Assisted Reaction Rate Constants, in cm^3 $molecule^{-1}$ s^{-1}, Calculated Using eq 3, as a Function of Temperature (Taking into Account 100% Relative Air Humidity at Each Temperature)

T (K)	k^{eff}(Ia)	k^{eff}(IIb)	$k^{overall}_{water\text{-}assisted}$
250	5.57×10^{-16}	1.24×10^{-14}	1.29×10^{-14}
260	5.48×10^{-16}	1.40×10^{-14}	1.45×10^{-14}
270	5.58×10^{-16}	1.58×10^{-14}	1.63×10^{-14}
280	5.48×10^{-16}	1.68×10^{-14}	1.73×10^{-14}
290	5.34×10^{-16}	1.73×10^{-14}	1.78×10^{-14}
300	5.31×10^{-16}	1.78×10^{-14}	1.83×10^{-14}
310	5.37×10^{-16}	1.85×10^{-14}	1.90×10^{-14}
320	5.49×10^{-16}	1.91×10^{-14}	1.96×10^{-14}
330	5.67×10^{-16}	1.98×10^{-14}	2.03×10^{-14}

order of magnitude. Thus only the HAT Ia path will be considered. For paths IIa and IIb (Figure 5), the situation is similar to the one encountered in the water-free reaction, in Figure 3: the water-assisted TS-IIa and TS-IIb are transformed into one another by rotation of the OH group around an incipient bond. Thus, in the overall rate constant kinetics calculation, the path with the largest rate constant (IIb) will be used. In Table 7, rate constants for the Ia and IIb reactions are added, and the total overall rate constant is equal to 1.90×10^{-14} cm^3 $molecule^{-1}$ s^{-1}. This quantity represents the contribution, to the total formic acid + OH reaction in a 100% humidity atmosphere, of the fraction of formic acid that is complexed with water. The carboxylic H-abstraction path contribution is negligible, while the formyl H-abstraction is the dominant pathway (97.44%).

The variation of paths Ia and IIb as a function of temperature is given in Table 8. The Ia path contribution is always practically negligible compared to IIb.

Finally, the total rate constant in the presence of water can be written as

$$k^{total} = k^{overall}_{water\text{-}free}(1 - X_{complex}) + k^{overall}_{water\text{-}assisted}$$

At 300 K, $X_{complex}$ is 0.12, and the contributions of the water-free and water-assisted rate constants are 3.86×10^{-13} (Table 5) and 1.83×10^{-14} cm^3 $molecule^{-1}$ s^{-1} (Table 8), respectively. Thus, the total rate constant, calculated as the weighed sum of the water-free and water-assisted rate constant fractions, is about 4.04×10^{-13} cm^3 $molecule^{-1}$ s^{-1}, which is about 8% slower than the rate constant in a dry atmosphere: 4.39×10^{-13} cm^3 $molecule^{-1}$ s^{-1}. This percent difference is approximately constant as a function of temperature, slightly decreasing as temperature increases.

CONCLUSIONS

In this work, we have calculated the formic acid + OH reaction rate constant, both in a dry atmosphere and in a 100% humidity environment, using the M05-2X density functional method and transition state theory computational kinetics. This method reproduces very accurately the experimental results.

We have determined the formic acid concentration that is normally complexed with water in the troposphere. We find that, at 300 K and 100% humidity, 12% of formic acid is found in the form of a water complex that is stabilized by two relatively strong hydrogen bonds. In fact, this complex is much more strongly bound than the water dimer.

One of the hydrogen bonds in the formic acid−water complex involves the carboxylic hydrogen atom, dramatically increasing the barrier for subsequent reaction with an OH radical. As a consequence, while in a dry atmosphere the formyl branching ratio represents about 16% of the overall rate constant, for the complexed fraction, the PCET mechanism becomes negligible and the formyl H-abstraction channel accounts for approximately 97% of the rate constant. Considering that abstraction of the formyl hydrogen is a much slower channel than the carboxyl H-abstraction, the overall rate coefficient is then slower than in the absence of water. However, since complexation accounts only for ∼12% of formic acid, this difference is negligible.

In previous work on the glyoxal and acetaldehyde water-assisted reactions with OH, we showed that one-water-molecule catalysis did not occur because the complex fraction was negligibly small (∼0.02%). In the case of formic acid, the complex fraction is much larger (12% at 300 K), but reaction occurs along a much slower channel. Thus, we show that water does not accelerate the reaction between formic acid and OH radicals under atmospheric conditions.

AUTHOR INFORMATION

Corresponding Author

*E-mail: ciuga@xanum.uam.mx (C.I.); jidaboy@unam.mx (J.R.A.-I.).

ACKNOWLEDGMENT

We thank Dr. Oksana Tishchenko, University of Minnesota, for valuable discussions. This work is a result of the FONCICYT Mexico-EU "RMAYS" network, Project No. 94666. It was partially supported by a grant from DGAPA UNAM (PAPIIT-IN203808). C.I. thanks the Instituto de Ciencia y Tecnología del D. F., México, for a postdoctoral fellowship. We gratefully acknowledge the Laboratorio de Visualización y Cómputo Paralelo at Universidad Autónoma Metropolitana—Iztapalapa and the Dirección General de Servicios de Cómputo Académico (DGSCA) at Universidad Nacional Autónoma de México for computer time.

REFERENCES

(1) (a) Iuga, C.; Alvarez-Idaboy, J. R.; Reyes, L.; Vivier-Bunge, A. *J. Phys. Chem. Lett.* **2010**, *1*, 3112. (b) Iuga, C.; Alvarez-Idaboy, J. R.; Vivier-Bunge, A. *Chem. Phys. Lett.* **2010**, *501*, 11. (c) Iuga, C.; Alvarez-Idaboy, J. R.; Vivier-Bunge, A. *Theor. Chem. Acc.* **2011**, *129*, 209.

(2) Vaida, V.; Headrick, J. E. *J. Phys. Chem. A* **2000**, *104*, 5401.

(3) Legrand, M.; de Angelis, M. *J. Geophys. Res.* **1995**, *100*, 1445.

(4) Grosjean, D. *Environ. Sci. Technol.* **1989**, *23*, 1506.

(5) Puxbaum, H.; Rosenberg, C.; Gregori, M.; Lanzerstorfer, C.; Ober, E.; Winiwarter, W. *Atmos. Environ.* **1988**, *22*, 1841.

(6) Sanhueza, E.; Santana, M.; Hermoso, M. *Atmos. Environ.* **1992**, *26A*, 1421.

(7) Granby, K.; Christensen, C. S.; Lohse, C. *Atmos. Environ.* **1997**, *31*, 1403.

(8) Kesselmeier, J. *J. Atmos. Chem.* **2001**, *39*, 219.

(9) Hanst, P. L.; Wong, N. W.; Bragin, J. *Atmos. Environ.* **1982**, *16*, 969.

(10) Keene, W. C.; Galloway, J. N.; Holden, J. D. *J. Geophys. Res.* **1983**, *88*, 5122.

(11) Wine, P. H.; Astalos, R. J.; Mauldin, R. L., III. *J. Phys. Chem.* **1985**, *89*, 2620.

(12) Zetzsch, C.; Stuhl, F. *Physico-Chemical Behavior of Atmospheric Pollutants. Proceedings of the Second European Symposium*; D. Reidel: Dordrecht, The Netherlands, 1982; p 129.

(13) Jolly, G. S.; McKenney, D. J.; Singleton, D. L.; Paraskevopoulos, G.; Bossard, A. R. *J. Phys. Chem.* **1986**, *90*, 6557.
(14) Singleton, D. L.; Paraskevopoulos, G.; Irwin, R. S.; Jolly, G. S.; McKenney, D. J. *J. Am. Chem. Soc.* **1988**, *110*, 7786.
(15) Dagaut, P.; Wallington, T. J.; Liu, R.; Kurylo, M. J. *Int. J. Chem. Kinet.* **1988**, *20*, 331.
(16) Galano, A.; Alvarez-Idaboy, J. R.; Ruiz-Santoyo, M. E.; Vivier-Bunge, A. *J. Phys. Chem. A* **2002**, *106*, 9520.
(17) Olivella, S.; Anglada, J. M.; Solé, A.; Bofill, J. M. *Chem.—Eur. J.* **2004**, *10*, 3404.
(18) Anglada, J. M. *J. Am. Chem. Soc.* **2004**, *126*, 9809.
(19) Benson, S. W. *Thermochemical Kinetics*, 2nd ed.; Wiley-Interscience: New York, 1976.
(20) Smith, I. W. M.; Ravishankara, A. R. *J. Phys. Chem. A* **2002**, *106*, 4798.
(21) Hansen, J. C.; Francisco, J. S. *ChemPhysChem* **2002**, *3*, 833.
(22) Alvarez-Idaboy, J. R.; Mora-Diez, N.; Boyd, R. J.; Vivier-Bunge, A. *J. Am. Chem. Soc.* **2001**, *123*, 2018.
(23) Torrent-Sucarrat, M.; Anglada, J. M. *ChemPhysChem* **2004**, *5*, 183.
(24) DeMore, W. B.; Sander, S. P.; Golden, D. M.; Hampson, R. F.; Kurylo, M. J.; Howard, C. J.; Ravishankara, A. R.; Kolb, C. E.; Molina, M. J. *JPL Publ.* **1997**, *97*, 4.
(25) Atkinson, R.; Baulch, D. L.; Cox, R. A.; Hampson, R. F., Jr.; Kerr, J. A.; Rossi, M. J.; Troe, J. *J. Phys. Chem. Ref. Data* **1999**, *28*, 191.
(26) Uc, V. H.; Alvarez-Idaboy, J. R.; Galano, A.; Vivier-Bunge, A. *J. Phys. Chem. A* **2008**, *112*, 7608.
(27) Åstrand, P. O.; Karlstrom, G.; Engdahl, A.; Nelander, B. *J. Chem. Phys.* **1995**, *102*, 3534.
(28) Rablen, P. R.; Lockman, J. W.; Jorgensen, W. L. *J. Phys. Chem. A* **1998**, *102*, 3782.
(29) Priem, D.; Ha, T. K.; Bauder, A. *J. Chem. Phys.* **2000**, *113*, 169.
(30) Luo, Y.; Maeda, S.; Ohno, K. *Chem. Phys. Lett.* **2009**, *469*, 57.
(31) Long, B.; Zhang, W.-j.; Tan, X.-f.; Long, Z.-w.; Wang, Y.-b.; Ren, D.-s. *Comput. Theor. Chem.* **2011**, *964*, 248.
(32) Zhao, Y.; Schultz, N. E.; Truhlar, D. G. *J. Chem. Theory Comput.* **2006**, *2*, 364.
(33) Zhao, Y.; Schultz, N. E.; Truhlar, D. G. *J. Chem. Theory Comput.* **2006**, *2*, 364.
(34) Zavala-Oseguera, C.; Alvarez-Idaboy, J. R.; Merino, G.; Galano, A. *J. Phys. Chem. A* **2009**, *113*, 13913.
(35) Velez, E.; Quijano, J.; Notario, R.; Pabón, E.; Murillo, J.; Leal, J.; Zapata, E.; Alarcón, G. *J. Phys. Org. Chem.* **2009**, *22*, 971.
(36) Vega-Rodriguez, A.; Alvarez-Idaboy, J. R. *Phys. Chem. Chem. Phys.* **2009**, *11*, 7649.
(37) Galano, A.; Alvarez-Idaboy, J. R. *Org. Lett.* **2009**, *11*, 5114.
(38) Black, G.; Simmie, J. M. *J. Comput. Chem.* **2010**, *31*, 1236.
(39) Furuncuoglu, T.; Ugur, I.; Degirmenci, I.; Aviyente, V. *Macromolecules* **2010**, *43*, 1823.
(40) Gao, T.; Andino, J. M.; Alvarez-Idaboy, J. R. *Phys. Chem. Chem. Phys.* **2010**, *12*, 9830.
(41) Galano, A.; Macías-Ruvalcaba, N. A.; Campos, O. N. M.; Pedraza-Chaverri, J. *J. Phys. Chem. B* **2010**, *114*, 6625.
(42) Eyring, H. *J. Chem. Phys.* **1935**, *3*, 107.
(43) Evans, M. G.; Polanyi, M. *Trans. Faraday Soc.* **1935**, *31*, 875.
(44) Truhlar, D. G.; Hase, W. L.; Hynes., J. T. *J. Phys. Chem.* **1983**, *87*, 2264.
(45) Duncan, W. T.; Bell, R. L.; Truong, T. N. *J. Comput. Chem.* **1998**, *19*, 1039.
(46) Zhang, S.; Truong, T. N. VKLab version 1.0, University of Utah, 2001.
(47) Eckart, C. *Phys. Rev.* **1930**, *35*, 1303.
(48) Galano, A.; Narciso-López, M.; Francisco-Márquez, M. *J. Phys. Chem. A* **2008**, *114*, 5796.
(49) Alvarez-Idaboy, J. R.; Galano, A. *Theor. Chem. Acc.* **2010**, *126*, 75.
(50) Wallnoefer, H. G.; Fox, T.; Liedl, K. R.; Tautermann, C. S. *Phys. Chem. Chem. Phys.* **2010**, *12*, 14941.
(51) Galano, A.; Alvarez-Idaboy, J. R. *J. Comput. Chem.* **2006**, *27*, 1203.
(52) Åstrand, P. O.; Karlstrom, G.; Engdahl, A.; Nelander, B. *J. Chem. Phys.* **1995**, *102*, 3534.
(53) Pfeilsticker, K.; Lotter, A.; Peters, C.; Bösch, H. *Science* **2003**, *300*, 2078.
(54) (a) Alvarez-Idaboy, J. R.; Mora-Diez, N.; Vivier-Bunge, A. *J. Am. Chem. Soc.* **2000**, *122*, 3715. (b) Mora-Diez, N.; Alvarez-Idaboy, J. R.; Boyd, R. J. *J. Phys. Chem. A* **2001**, *105*, 9034. (c) Uc, V. H.; Alvarez-Idaboy, J. R.; Galano, A.; Garcia-Cruz, I.; Vivier-Bunge, A. *J. Phys. Chem. A* **2006**, *110*, 10155. (d) Francisco-Marquez, M.; Alvarez-Idaboy, J. R.; Galano, A.; Vivier-Bunge, A. *Phys. Chem. Chem. Phys.* **2003**, *5*, 1392. (e) Galano, A. *J. Phys. Chem. A* **2006**, *110*, 9153.